(s, doublet of triplets after selective decoupling of aromatic protons, $^2J(PH)$ = 12 Hz, ($^3J(PH)$ = 10 Hz, PPh_3). $^{13}C\{^1H\}$ NMR (CD_2Cl_2): δ 173.5 (t, $J(PC)$ = 7.0 Hz, Ir-CO), [133.4 (t, $J(PC)$ = 5.6 Hz), 131.6 (s), 129.3 (t, $J(PC)$ = 30 Hz), 128.9 (t, $J(PC)$ = 5.3 Hz) (PPh_3)].

(b) Thermal Rearrangement of 3. A pale yellow solution of 3 (0.150 g, 0.145 mmol) in CH_2Cl_2/benzene (15 mL, 1:2 v/v) was stirred under reflux for 22 h. The resulting yellow-brown solution was taken to dryness, the solid residue dissolved in CH_2Cl_2 (5 mL), and diethyl ether added to afford a pale yellow powder (0.110 g). The IR (mineral oil mull) spectrum of the solid showed the residual ν(CO) absorption band of 3, together with new bands at ca. 2200 (br w) and 2040 (s) cm^{-1}, assigned to complex 5. ^1H and ^{31}P NMR analyses showed the presence of 3 and 5 in almost equimolar amounts.

X-ray Structure Study. Diffraction data for compound 3 were collected on a Siemens R3m/v four-circle diffractometer using a graphite-monochromated Mo Kα (λ = 0.71073 Å) radiation and an ω-scan technique. Accurate unit cell dimensions and crystal orientation matrices were obtained from least-squares refinement of 25 strong reflections in the $15 < 2\theta < 30$ range. Lorentz and polarization corrections were applied to the intensity data. An absorption correction was applied (DIFABS[32]). The structure was solved by using standard Patterson methods and subsequently by using Fourier maps. All non-hydrogen atoms were refined anisotropically, while hydrogen atoms of the methyl group (from a ΔF map) and other hydrogen atoms (from calculated positions) were included with a common thermal parameter (U = 0.08 Å^2). Of 11 136 reflections there were 9279 unique and 6511 with $I > 3\sigma(I)$. These data were used in the final refinement of the structural parameters to arrive at residuals of R = 0.059 and R_w = 0.061. The weighting scheme used in the last refinement cycle was $w = 1.0000/\sigma(F_o)^2 + 0.001(F_o)^2$. All calculations were performed by using the SHELTX PLUS (version 3.43)[33] and PARST[34] computer programs.

Acknowledgment. We thank the Italian Ministero dell'Università e della Ricerca Scientifica e Tecnologica for funding and the Johnson-Matthey Research Centre, Reading, England, for the loan of iridium metal. We also thank Prof. M. Longeri for obtaining the NMR spectra and helpful discussions.

Supplementary Material Available: Complete listings of bond distances, angles, atomic coordinates, and anisotropic thermal parameters (6 pages); a listing of observed and calculated structure factors (34 pages). Ordering information is given on any current masthead page.

(32) Walker, N.; Stuart, D. *Acta Crystallogr., Sect. A* **1983**, *A39*, 158.
(33) *SHELXTL PLUS Version 3.43*; Siemens Analytical X-Ray Instruments Inc.: Madison, WI, 1989.
(34) Nardelli, M. *Comput. Chem.* **1983**, *7*, 95.

Small Heteroborane Cluster Systems. 1.[1] Theoretical Study of Bridged and Cage-Inserted Phosphaborane Cluster Compounds with Semiempirical Molecular Orbital Calculations

John A. Glass, Jr., Thomas A. Whelan,[†] and James T. Spencer*

Department of Chemistry and Center for Molecular Electronics, Center for Science and Technology, Syracuse University, Syracuse, New York 13244-4100

Received August 29, 1990

The structural, thermodynamic, and electronic properties of 91 phosphaborane cluster compounds have been calculated by using the MNDO-SCF semiempirical molecular orbital calculational method. The geometry-optimized minimum energy structures for all the known, structurally characterized phosphaborane systems have been calculated, and exceptionally good agreement between experimentally determined and calculated structural parameters has been observed. Calculations for five classes of small phosphaborane clusters, with fewer than nine vertex atoms, have been completed and have been related to experimentally and spectroscopically proposed structural types. The relationship between bridged and inserted phosphaborane structures has been related to the variation in molecular orbital energies as a function of the (phosphorus-bridged boron atom plane)-(basal boron plane) dihedral angle. Complete MO correlation diagrams that relate the orbitals for bridged phosphaborane systems to inserted systems have been constructed. Linear relationships have been observed between the calculated charge on the phosphorus atom and both the phosphorus-apical boron bond distance and the bridgehead basal boron bond distance. The hydrogen atoms bridging basal boron atoms in the phosphorus-inserted clusters were found to be deflected toward the boron atoms bonded to the phosphorus. The boron atoms bonded to the phosphorus atom, therefore, more closely resemble BH_2 units with two terminal protons rather than BH units that contain only one terminal proton each. Predictions concerning structural and chemical reactivities for unknown phosphaborane compounds have been made on the basis of these MO calculations.

Introduction

It has become clearly evident that borane and heteroborane clusters and their transition-metal complexes bear close electronic and structural relationships with other main-group and organometallic clusters and that experimental and theoretical insights gained from the study of these boron caged systems can be profitably extended to other classes of molecular polyhedra.[2,3] The theoretical study of heteroborane cluster species by semiempirical

[†]Current Address: Department of Chemistry, State University of New York, College at Potsdam, Potsdam, NY 13676.

(1) Part 2: Miller, R. W.; Donaghy, K. J.; Spencer, J. T. *Organometallics*, following paper in this issue.
(2) Wade, K. *Inorg. Chem. Radiochem.* **1976**, *18*, 1.
(3) Lipscomb, W. N. *Inorg. Chem.* **1979**, *18*, 2328.

0276-7333/91/2310-1148$02.50/0

molecular orbital calculational methods provides a valuable tool for the exploration of the fundamental nature of these species. Questions concerning the bonding roles and interactions of lone-pair electrons on a heteroatom, relative stabilities of related cluster geometries, and the elucidation of factors that are important in determining cluster geometries, stabilities, and reactivities can be effectively studied with these calculations. The heteroatom reaction chemistry reported in subsequent papers in this series[1,4] has been largely predicted and guided by the calculations reported here. As an example, the chemical inaccessibility of the lone pair of electrons on the phosphorus for external coordination in bridged $R_2PB_5H_8$ compounds was predicted on the basis of the internal charge distribution and the calculated involvement of the lone pair in cage bonding. Of particular interest are the phosphaborane systems, since these species serve as good models for a wide variety of heteroatom-substituted cluster species. In addition, nine of the large phosphaborane systems have been characterized structurally by diffraction experiments.[5-12] These systems provide convenient benchmarks with which to evaluate the validity of the application of the calculational method to related structurally unknown and chemically interesting systems.

The MNDO (modified neglect of differential overlap) semiempirical method of Dewar[13] has been extensively employed in these calculations. MNDO has been shown to provide superior structural and thermodynamic data for boron hydride and heteroborane systems.[14-19] Only a single phosphaborane MNDO calculation has been reported, 1,2-$PCB_{10}H_{11}$.[16a] The gas-phase photoelectron spectrum of this compound was found to agree remarkably well with the results of the MNDO calculation. Onak has recently shown the utility of MNDO calculations in correctly predicting the relative orders of stability of a wide variety of *closo*-RR'-2,4-$C_2B_5H_5$ systems (R = R' = H; R = H, R' = Cl, Br, I, C_2H_5, Me_3N (3 isomers each); R = R' = *closo*-$RC_2B_4H_5$ (5 isomers each); R = H, R' = 2,4-$C_2B_5H_6$ (6 isomers); R = Cl, R' = *B,B'*-(C_2H_5)-*closo*-$C_2B_5H_4$ (11 isomers)) with very few predictive exceptions.[16b]

In this work, we have explored the use of the MNDO–SCF semiempirical calculational method in the systematic study of a wide variety of phosphaborane cluster systems, both those that are structurally known and those whose structures are yet unknown. We have also investigated the relationship between bridged and inserted phosphaborane systems in polyhedral borane cluster systems.

Experimental Section

The MNDO (modified neglect of differential overlap) calculations employed in this work were peformed with either version 4.01 or 5.02 of MOPAC[20,21] on either a Hewlett-Packard Series 800 computer system in the Center for Molecular Electronics at Syracuse University or the VAX 8820 system of the Syracuse University Academic Computing Services, respectively. Except where noted, all calculations were free varied and run with the PRECISE[22] option employed. The procedure used to find the MNDO-optimized minimum energy geometries on the potential energy surface for the phosphaborane systems reported here utilized several steps. The starting input geometry of the compound was approximated on the basis of appropriate substitutions of an estimated parent structure. The parent structure used for all B_5 systems was that of a pentagonal-pyramidal structure, similar to the structure of *nido*-B_6H_{10}.[23,24] Calculations for class I and II compounds (Scheme I) were allowed to freely vary with only the constrains of an overall C_s molecular symmetry applied (except as discussed below) to locate the stationary point on the potential energy surface. In most cases, the structure optimized without symmetry restrictions. In compounds in which the substituent groups on the phosphorus had large steric requirements, however, the symmetry restrictions were required to keep the basal boron atoms attached to the phosphorus from migrating away from the non-phosphorus-bridged basal boron atoms of the cage. Compounds belonging to classes III–V (Schemes III and V) had the symmetry restriction imposed in order to obtain an inserted phosphaborane cluster structure. In cases where the initial geometry did not lead to an optimized structure, the final MNDO output geometry was reinput into the calculation and run again until a MNDO optimization was achieved. In most cases, this was realized in fewer than five calculations. The four chromium complexes did not, however, optimize even after repeated calculations. The structures of these complexes were, however, consistent with those expected on the basis of the structure of the free phosphaborane cage and normal organometallic and known chromium metallaborane structural considerations.[25]

Of particular interest was the relationship between bridged and inserted structures for related classes of phosphaborane compounds (classes I–III and classes II–IV conversions). In these calculations, the starting bridged structure used the same input geometry as was employed for compounds **9** or **26**. The (apical boron)–(basal plane centroid)–(phosphorus atom) angle was, however, restricted in the calculation. The structure was then optimized consistent with an overall C_s molecular symmetry. In subsequent calculations, the restricted B(1)–centroid–P angle was systematically varied from 150 to 75° in 5° increments and the

(4) The reaction chemistry of phosphaalkynes with borane cluster systems: Miller, R. W.; Spencer, J. T. Submitted for publication.
(5) Friedman, L. B.; Perry, S. L. *Inorg. Chem.* **1973**, *12*, 288.
(6) Haubold, W.; Keller, W.; Sawitzki, G. *Angew. Chem., Int. Ed. Engl.* **1988**, *27*, 925.
(7) Todd, L. J.; Paul, I. C.; Little, J. L.; Welcker, P. S.; Peterson, C. R. *J. Am. Chem. Soc.* **1968**, *90*, 4489.
(8) Mastryukov, V. S.; Atavin, E. G.; Vilkov, L. V.; Golubinskii, A. V.; Kalinin, V. N.; Zhigareva, G. G.; Zakharkin, L. I. *J. Mol. Struct.* **1979**, *56*, 139.
(9) Wong, H. S.; Lipscomb, W. N. *Inorg. Chem.* **1975**, *14*, 1350.
(10) Getman, T. D.; Deng, H.-B.; Hsu, L.-Y.; Shore, S. G. *Inorg. Chem.* **1989**, *28*, 3612.
(11) Little, J. L.; Kester, J. G.; Huffman, J. C.; Todd, L. J. *Inorg. Chem.* **1989**, *28*, 1087.
(12) Thornton-Pett, M.; Beckett, M. A.; Kennedy, J. D. *J. Chem. Soc., Dalton Trans.* **1986**, 303.
(13) Dewar, M. J. S.; Theil, N. *J. Am. Chem. Soc.* **1977**, *99*, 5231.
(14) Dewar, M. J. S.; McKee, M. L. *Inorg. Chem.* **1978**, *17*, 1569.
(15) Ulman, J. A.; Fehlner, T. P. *J. Am. Chem. Soc.* **1978**, *100*, 449.
(16) (a) Brint, P.; Sangchakr, B.; McGrath, M.; Spalding, T.; Suffolk, R. J. *Inorg. Chem.* **1990**, *29*, 47. (b) Onak, T.; O'Gorman, E.; Banuelos, T.; Alfonso, C.; Yu, M. *Inorg. Chem.* **1990**, *29*, 335.
(17) Maguire, J. A.; Ford, G. P.; Hosmane, N. S. *Inorg. Chem.* **1988**, *27*, 3354.
(18) Andersen, E. L.; DeKock, R. L.; Fehlner, T. P. *J. Am. Chem. Soc.* **1980**, *102*, 2644.
(19) O'Gorman, E.; Banuelos, T.; Onak, T. *Inorg. Chem.* **1988**, *27*, 912.
(20) Parametrizations used for the MNDO calculations were: (a) Dewar, M. J. S.; McKee, M. L. *J. Am. Chem. Soc.* **1977**, *99*, 5231. (b) Dewar, M. J. S.; Theil, W. *J. Am. Chem. Soc.* **1977**, *99*, 4899. (c) Dewar, M. J. S.; McKee, M. L.; Rzepa, H. S. *J. Am. Chem. Soc.* **1978**, *100*, 3607. (d) Dewar, M. J. S.; Friedheim, J.; Grady, G.; Healy, E. F.; Stewart, J. J. P. *Organometallics* **1986**, *5*, 375. (e) Dewar, M. J. S.; Rzepa, H. S. *J. Comput. Chem.* **1983**, *4*, 158.
(21) Stewart, J. J. P.; Seiler, F. J. *Quantum Chem. Program Exch.* Program No. 455.
(22) Boyd, D. B.; Smith, D. W.; Stewart, J. J. P.; Wimmer, E. J. *J. Comput. Chem.* **1988**, *9*, 387.
(23) Eriks, K.; Lipscomb, W. N.; Schaeffer, R. *J. Chem. Phys.* **1954**, *22*, 754.
(24) Hirshfeld, F. L.; Eriks, K.; Dickerson, R. E.; Lippert, E. L., Jr.; Lipscomb, W. N. *J. Chem. Phys.* **1958**, *28*, 56.
(25) (a) Kirtley, S. W. In *Comprehensive Organometallic Chemistry*; Wilkinson, G., Stone, F. G. A., Abel, E., Eds.; Pergamon: Oxford, England, 1982; Vol. 3, Chapter 26.1, p 783. (b) Davis, R.; Kane-Maguire, L. A. P. In *Comprehensive Organometallic Chemistry*; Wilkinson, G., Stone, F. G. A., Abel, E., Eds; Pergamon: Oxford, England, 1982; Vol. 3, Chapter 26.2, p 953. (c) Hawthorne, M. F.; Young, D. C.; Andrews, T. D.; Howe, D. V.; Pilling, R. L.; Pitts, A. D.; Reintjes, M.; Warren, L. F., Jr.; Wegner, P. A. *J. Am. Chem. Soc.* **1968**, *90*, 879. (d) Hawthorne, M. F.; Dunks, G. B. *Science* **1972**, *178*, 462. (e) Hawthorne, M. F. *Pure Appl. Chem.* **1972**, *29*, 547. (f) Francis, J. N.; Hawthorne, M. F. *Inorg. Chem.* **1971**, *10*, 863. (g) St. Clair, D.; Zalkin, A.; Templeton, D. H. *Inorg. Chem.* **1971**, *10*, 2587.

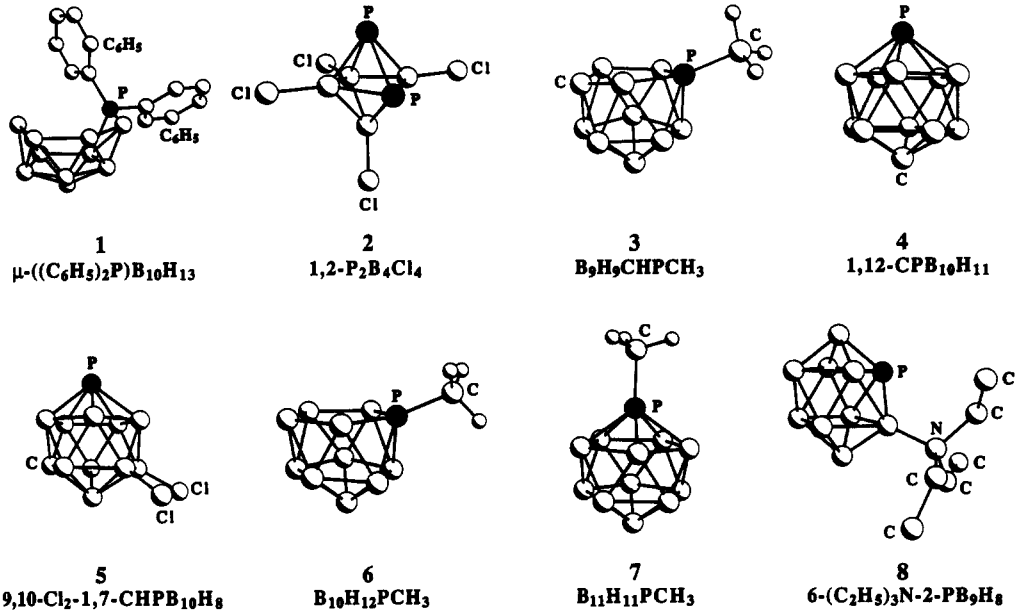

1 μ-((C$_6$H$_5$)$_2$P)B$_{10}$H$_{13}$ | 2 1,2-P$_2$B$_4$Cl$_4$ | 3 B$_9$H$_9$CHPCH$_3$ | 4 1,12-CPB$_{10}$H$_{11}$

5 9,10-Cl$_2$-1,7-CHPB$_{10}$H$_8$ | 6 B$_{10}$H$_{12}$PCH$_3$ | 7 B$_{11}$H$_{11}$PCH$_3$ | 8 6-(C$_2$H$_5$)$_3$N-2-PB$_9$H$_8$

Figure 1. Structurally characterized phosphaborane systems. Hydrogen atoms have been omitted for clarity (except for CH_3 groups).

structures were again optimized consistent with C_s symmetry. In the construction of Figures 4 and 9, these B(1)–centroid–P angles were converted into the dihedral angles between the basal boron plane and the bridging B(2)–P–B(3) plane. Orbital assignments and connectivities were made by inspection of the atomic orbital coefficients of the LCAO set for each MO. Interactions between the filled and virtual orbitals were not considered. In all cases, assignments of the orbitals at various angles was straightforward. In most cases the noncrossing rule was observed in assigning group orbital connectivities with apparent violations of this rule due to the introduction of significant degrees of orbital mixing at intermediate positions.

The molecular orbital correlation diagrams shown in Figures 2 and 7 were constructed by using the group orbital approach.[26] Orbital connectivities and symmetries were assigned by inspection of the MNDO-generated LCAO contributions to each MO. Calculations of the phosphorus group fragments, $+PH_2$ and $+PCH_2$, were allowed to fully optimize without restriction. As above, the noncrossing rule was generally observed with apparent violations due to significant orbital mixing.

The correlation data between the calculated charge on the phosphorus atom and the phosphorus–apical boron and the B(2)–B(3) bond distances for class I systems (Figure 5) were obtained by sequentially substituting halogen atoms for hydrogens of the exopolyhedral methyl groups of compound **10**. In each case the calculation was optimized as describe above.

In the fully optimized calculations for class III compounds, the hydrogen atoms bridging between boron atoms B(3)–B(4) and B(2)–B(5) (Scheme II) were found to be deflected toward boron atoms B(3) and B(2), respectively. The boron atoms that are bonded to the phosphorus atom, therefore, more closely resembled a BH_2 unit with two terminal protons than a BH unit that contains only one terminal proton. An investigation was undertaken to determine the effect of this proton shift on the calculated structures and orbital energies. Compound **43** was selected as the model compound for these calculations. The geometry of the phosphaborane cage was first established through a complete geometry-optimized calculation with no symmetry restrictions except the requirement that the phosphorus atom be restricted to the basal plane. The positions of the bridging hydrogen atoms were then fixed relative to the centroid of the basal plane and the structure optimized as was done for compound **43**. The positions of the hydrogen atoms were systematically varied from calculation to calculation by incrementing ($\leq 2°$) the (hydrogen)–(basal plane centroid)–(phosphorus atom) angle from 58 to 140° (Figures 10 and 11). Each structure was then optimized consistent with an overall C_s symmetry. One overall ΔH_f minimum was observed with two very shallow higher energy inflections corresponding to the three structural extremes, respectively (a) the structure with the two hydrogen atoms shifted toward boron atoms B(2) and B(3), (b) the symmetrically bridged structure, and (c) the structure in which the hydrogens have shifted toward boron atoms B(4) and B(5).

(26) Clark, T. In *A Handbook of Computational Chemistry. A Practical Guide to Chemical Structure and Energy Calculations*; Wiley: New York, 1985.

Results and Discussion

Structurally Characterized Phosphaborane Systems. In order to establish the validity and accuracy of the MNDO calculational method for phosphaborane cluster systems, the geometry-optimized calculations of all the known, structurally characterized phosphaborane systems were undertaken first. Most of the synthetic experimental work reported thus far with phosphaborane clusters involves compounds with more than nine vertex atoms. These systems are predominantly based on an icosahedral parent structure. Nine phosphaboranes have been crystallographically characterized,[5-12] and these are shown in Figure 1 (only the 5,6-isomer of the bridging (diphenylphosphino)decaborane system is shown although both the 5,6- and 6,9-isomers were calculated). Several other large phosphaborane and phosphacarborane systems have been reported, both as free clusters[27-35] and as their transition-metal complexes,[29,36-43] but structural data for

(27) Todd, L. J.; Little, J. L.; Silverstein, H. T. *Inorg. Chem.* **1969**, *8*, 1698.
(28) Little, J. L. *Inorg. Chem.* **1976**, *15*, 114.
(29) Little, J. L.; Wong, A. C. *J. Am. Chem. Soc.* **1971**, *93*, 522.
(30) Little, J. L.; Moran, J. T.; Todd, L. J. *J. Am. Chem. Soc.* **1967**, *89*, 5495.
(31) Smith, H. D.; Knowles, T. A.; Schroeder, H. *Inorg. Chem.* **1965**, *4*, 107.
(32) Todd, L. J.; Burke, A. R.; Garber, A. R.; Silverstein, H. T.; Storhoff, B. N. *Inorg. Chem.* **1970**, *9*, 2175.
(33) Alexander, R. P.; Schroeder, H. *Inorg. Chem.* **1963**, *2*, 1107.
(34) Alexander, R. P.; Schroeder, H. *Inorg. Chem.* **1966**, *5*, 493.
(35) Maruca, R. *Inorg. Chem.* **1970**, *9*, 1593.
(36) Silverstein, H. T.; Beer, D. C.; Todd, L. J. *J. Organomet. Chem.* **1970**, *21*, 139.
(37) Welcker, P. S., Todd, L. J. *Inorg. Chem.* **1970**, *2*, 286.
(38) Little, J. L.; Welcker, P. S.; Loy, N. J.; Todd, L. J. *Inorg. Chem.* **1970**, *9*, 63.
(39) Smith, H. D., Jr. *J. Am. Chem. Soc.* **1965**, *87*, 1817.
(40) Beer, D. C.; Todd, L. J. *J. Organomet. Chem.* **1972**, *36*, 77.

Table I. Calculated (MNDO) and Experimental (X-ray) Structural Data (in Å) for Bridged and Inserted Phosphaborane Systems

	compd (type)											
	1 (bridged) μ-$((C_6H_5)_2P)B_{10}H_{13}$			2 (inserted) 1,2-$P_2B_4Cl_4$			3 (inserted) $Fe(B_9H_9CHPCH_3)_2$			4 (inserted) 1,12-$CPB_{10}H_{11}$		
	calcd	exptl[a]	Δ	calcd	exptl[b]	Δ	calcd[c]	exptl[d]	Δ	calcd	exptl[e,f]	Δ
bond												
P(1)-P(2)				2.14	2.22	−0.08						
B-P av	1.94	1.94	0.00	2.00	1.93	0.07	1.93[g]	1.90	0.03	2.01	2.05	−0.04
μ-B-(P)-B	2.46	2.69	−0.23									
B(4)-B(6)				1.73	1.67	0.06						
B-Cl av				1.75	1.75	0.00						
B-B av	1.93	1.87[h]	0.06	1.83	1.85	−0.02	1.80	1.81[i]	−0.01	1.86	1.87	−0.01
B-B′ av	1.78	1.74[h]	0.04				1.88	1.81[i]	0.07	1.80	1.79	0.01
B′-B′ av	1.82	1.83	−0.01				1.81	1.81[i]	0.00	1.83	1.79	0.04
B′-B″ av							1.82	1.81[i]	0.01			
C-B av							1.59	1.71[i]	−0.12			
C-B′ av							1.78	1.71[i]	0.07	1.76	1.69	0.07
C-B″ av												
P-C	1.75	1.78	−0.03				1.77	1.80	−0.03			
R factor		0.102			0.073			0.135			NR	
av |Δ|			0.06			0.05			0.04			0.03
ΔH_f, kJ mol^{-1}	250.6			−367.5			−20.8			−107.5		
IP, eV	9.88			11.07			9.26			12.30		
ref		5, 12			6			7			8	

	compound (type)											
	5 (inserted) 9,10-Cl_2-1,7-$CHPB_{10}H_8$			6 (inserted) $B_{10}H_{12}PCH_3$			7 (inserted) $B_{11}H_{11}PCH_3$			8 (inserted) 6-$(C_2H_5)_3N$-2-PB_9H_8		
	calcd	exptl[j]	Δ	calcd	exptl[k]	Δ	calcd	exptl[l]	Δ	calcd	exptl[m]	Δ
bond												
P(1)-P(2)												
B-P av	2.01	2.02	−0.01	2.00	1.99	0.01	2.03	1.95	0.08	2.05	1.94	0.11
μ-B-(P)-B												
B(4)-B(6)												
B-Cl av	1.80	1.79	0.01									
B-B av	1.84	1.82	0.02	1.86	1.88	−0.02	1.97	1.87	0.10	1.87	1.86	0.01
B-B′ av	1.82	1.77	0.05	1.86	1.78	0.08	1.77	1.79	−0.01	1.83	1.85	−0.02
B′-B′ av	1.84	1.79	0.05	1.82	1.81	0.01	1.85	1.79	0.06	1.80	1.77	0.03
B′-B″ av	1.83	1.79	0.04	1.81	1.76	0.05	1.82	1.76	0.06			
C-B av	1.73	1.71	0.02									
C-B′ av	1.77	1.73	0.04									
C-B″ av	1.76	1.75	0.01									
P-C				1.77	1.81	−0.04	1.78	1.77	0.01			
B-N										1.62	1.59	0.03
R factor		0.081			0.046			0.066			0.079	
av |Δ|			0.03			0.04			0.06			0.04
ΔH_f, kJ mol^{-1}	−255.7			−104.4			−204.2			103.3		
IP, eV	11.21			10.99			11.81			9.91		
ref		9			10			10			11	

[a] 5,6-isomer.[5] Atom labeling scheme: B = B(5,6,7,8,9,10); B′ = B(1,2,3,4). [b] Atom labeling scheme: B = B(3,4,5,6). [c] Calculated for B_9H_9CHPMe ligand uncomplexed to the iron atom. [d] Atom labeling scheme (phosphorus in the 7-position): B = B(8,10,11); B′ = B(2,3,4,5,6); B″ = B(1). [e] Gas-phase structure by electron diffraction. [f] Atom-labeling scheme (phosphorus in the 1-position): B = B(2,3,4,5,6); B′ = B(7,8,9,10,11). [g] Between the phosphorus and boron atoms in the basal plane (B atoms). [h] Excluding interactions with the two boron atoms involved in the B-P-B bond. [i] Only average B-B and C-B bond distances were reported without fractional atomic coordinates. [j] Atom labeling scheme (phosphorus in the 1-position): B = B(2,3,4,5,6); B′ = B(8,9,10,11); B″ = B(12). [k] Atom labeling scheme (phosphorus in the 7-position): B = B(8,9,10,11); B′ = B(2,3,4,5,6); B″ = B(1). [l] Atom labeling scheme (phosphorus in the 1-position): B = B(2,3,4,5,6); B′ = B(7,8,9,10,11); B″ = B(12). [m] Atom labeling scheme (phosphorus in the 2-position): B = B(1,3,5,6,9); B′ = B(4,7,8,10).

these compounds have not appeared in the literature. These structurally uncharacterized systems are expected to have structures very similar to those crystallographically characterized, on the basis of spectroscopic data. Beside the large cluster compounds, very little work has thus far been reported for other phosphaboranes. The only small systems that are known are several μ-phosphinopentaborane compounds reported independently by Burg,[44-46] Gaines,[47] and Spencer,[1] the *closo*-$P_2B_4Cl_4$ system,[48] and a proposed inserted phosphahexaborane compound reported by Gaines.[47] The only example of these smaller systems that has been structurally characterized is *closo*-$P_2B_4Cl_4$ (**2**).

The data for the MNDO-calculated structures for all the structurally characterized phosphaborane systems are presented in Table I. In each case, the calculated structural data are compared with the data from the crystal-

(41) Beer, D. C.; Todd, L. J. *J. Organomet. Chem.* **1973**, *55*, 363.
(42) Storhoff, B. N.; Infante, A. J. *J. Organomet. Chem.* **1975**, *84*, 291.
(43) Yamamoto, T.; Todd, L. J. *J. Organomet. Chem.* **1974**, *67*, 75.
(44) Burg, A. B. *Inorg. Chem.* **1973**, *12*, 3017.
(45) Burg, A. B.; Heinen, H. *Inorg. Chem.* **1968**, *7*, 1021.
(46) Mishra, I. B.; Burg, A. B. *Inorg. Chem.* **1972**, *11*, 664.
(47) Coons, D. E.; Gaines, D. F. *Inorg. Chem.* **1987**, *26*, 1985.
(48) Haubold, W.; Keller, W.; Sawitzki, G. *Angew. Chem., Int. Ed. Engl.* **1988**, *27*, 925.

Scheme I. Bridged Phosphaborane Systems

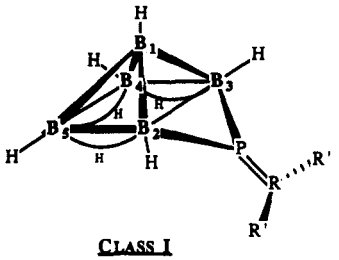

CLASS I

9	R = C;	R' = H;	Charge = 0
10	R = C;	R' = CH_3;	Charge = 0
11	R = C;	R' = CH_3, CH_2F;	Charge = 0
12	R = C;	R' = CH_3, CH_2Cl;	Charge = 0
13	R = C;	R' = CH_2F, CH_2F;	Charge = 0
14	R = C;	R' = CH_2Cl, CH_2Cl;	Charge = 0
15	R = C;	R' = CH_2F, CHF_2;	Charge = 0
16	R = C;	R' = CH_2Cl, $CHCl_2$;	Charge = 0
17	R = C;	R' = CHF_2, CHF_2;	Charge = 0
18	R = C;	R' = $CHCl_2$, $CHCl_2$;	Charge = 0
19	R = C;	R' = CHF_2, CF_3;	Charge = 0
20	R = C;	R' = $CHCl_2$, CCl_3;	Charge = 0
21	R = C;	R' = CF_3;	Charge = 0
22	R = C;	R' = CCl_3;	Charge = 0
23	R = C;	R' = C_6H_5;	Charge = 0
24	R = C;	R' = $Si(CH_3)_3$;	Charge = 0
25	R = C;	R' = H; $Cr(CO)_3$	Charge = 0

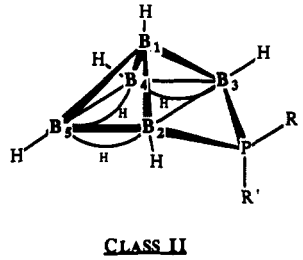

CLASS II

26	R = H;	R' = H;	Charge = 0
27	R = CH_3;	R' = CH_3;	Charge = 0
28a	R = CH_3;	R' = CD_3;	Charge = 0
28b	R = CD_3;	R' = CH_3;	Charge = 0
29	R = CF_3;	R' = CF_3;	Charge = 0
30a	R = H;	R' = F;	Charge = 0
30b	R = F;	R' = H;	Charge = 0
31a	R = H;	R' = Cl;	Charge = 0
31b	R = Cl;	R' = H;	Charge = 0
32	R = F;	R' = F;	Charge = 0
33	R = Cl;	R' = Cl;	Charge = 0
34a	R = Cl;	R' = CH_3;	Charge = 0
34b	R = CH_3;	R' = Cl;	Charge = 0
35a	R = Cl;	R' = C_6H_5	Charge = 0
35b	R = C_6H_5;	R' = Cl	Charge = 0
36a	R = Cl;	R' = $C(H)(C_6H_5)_2$;	Charge = 0
36b	R = $C(H)(C_6H_5)_2$;	R' = Cl;	Charge = 0
37a	R = Cl;	R' = $C(H)(SiMe_3)_2$;	Charge = 0
37b	R = $C(H)(SiMe_3)_2$;	R' = Cl;	Charge = 0
38	R = nothing;	R' = $C(^tBu)(H)(OSiMe_3)$;	Charge = -1
39a	R = $SiMe_3$;	R' = $C(^tBu)(H)(OSiMe_3)$;	Charge = 0
39b	R = $C(^tBu)(H)(OSiMe_3)$;	R' = $SiMe_3$;	Charge = 0
40a	R = H;	R' = $C(^tBu)(H)(OSiMe_3)$;	Charge = 0
40b	R = $C(^tBu)(H)(OSiMe_3)$;	R' = H;	Charge = 0
41a	R = H;	R' = $C(^tBu)(H)(OSiMe_3)$;	Charge = -1
41b	R = $C(^tBu)(H)(OSiMe_3)$;	R' = H;	Charge = -1
42	R = H;	R' = H; $Cr(CO)_3$	Charge = 0

Planes: Plane 1 = B(2), B(3), B(4), B(5)
Plane 2 = B(2), P, B(3)
Plane 3 = P, R,R'
Plane 4 = B(1), B(2), B(3)

lographically determined structure. In Figure 1 are shown the 3-dimensional drawings of the calculated optimized geometries for these compounds, 1–8. In general, exceptionally good agreement between the calculated and the experimentally determined parameters was found, with an average difference between the experimental and calculated bond lengths of $\Delta = 0.04$ Å (Δ = calculated value – experimental value). Both the experimentally determined and calculated bond lengths involving the phosphorus atoms in these systems are remarkably consistent (average P–B bond length, calculated = 2.00 Å and experimental = 1.97 Å with s (standard deviation) = 0.047 Å; average P–C bond length, calculated = 1.77 Å and experimental = 1.79 Å with s = 0.016 Å). The greatest difference between a calculated and an experimental structure was observed in the case of the bridged 5,6-$((C_6H_5)_2P)B_{10}H_{13}$ structure. In this structure, a significant underestimation of the B–B bond length bridged by the phosphino group was observed in the calculation (0.23 Å). This underestimation of the B–B bond length is a result of severe steric crowding encountered in the structure between the phenyl groups on the phosphorus atom and the framework atoms of the decaborane cage. This steric crowding problem is not encountered in the 6,9-isomer. Experimentally, a significant stability difference between the two isomers has been observed with the 5,6-nido-isomer rapidly converting to the 6,9-arachno-isomer on deprotonation of the cage.[12,49] In these decaborane-derived compounds and in compound 3, $Fe(B_9H_9CHPCH_3)_2$, the moderate quality of the experimental crystal structures (R = 0.102 for compound 1 (5,6-isomer) and R = 0.135 for compound 3) could additionally be contributing to the variation observed between the calculated and experimentally determined structures. Additionally, in the calculations for compound 3, the free phosphaborane cage was calculated rather than the metal

(49) Beckett, M. A.; Kennedy, J. D. *J. Chem. Soc., Chem. Commun.* **1983**, 575.

Scheme II. Synthetic Relationships between Class I and II Phosphaborane Systems

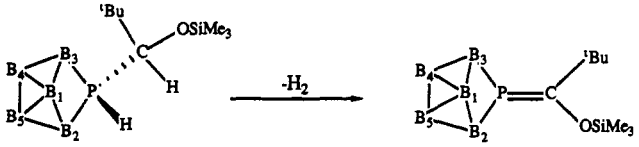

complex reported in the literature, since MNDO is not parametrized, in general, for transition metals. There was, however, excellent agreement between the final calculated structure of the free ligand and that reported for the cage in the iron complex. Finally, the reported structure for compound 4 is from a gas-phase electron diffraction study and the difference between the calculated and experimental structures is, as expected, the smallest observed for the known compounds (Δ = 0.03 Å). The strikingly good agreement between the calculated and the experimentally determined structures provides clear evidence of the utility of the MNDO method for investigating phosphaborane systems.

Small Phosphaborane Systems. The success of the MNDO method above in duplicating important structural features and providing electronic information for the larger phosphaborane systems clearly demonstrates the potential of the MNDO method in the study of the structurally unknown small phosphaborane compounds. Five classes of small phosphaboranes were studied in the calculations reported here. Each class was chosen to provide information on either known or proposed structural types of small phosphaborane systems, on the basis of spectroscopic analyses. Classes I and II represent bridging $B_5H_8P{=}CR_2$ and $B_5H_8PR_2$ compounds, respectively, and are shown in Scheme I. Structural data for selected compounds are reported in Table II, and thermodynamic and electronic data from the calculations are given in Table III. We have reported in the accompanying paper the synthesis and characterization of the only known example of a class I

Scheme III. Inserted Phosphaborane Systems

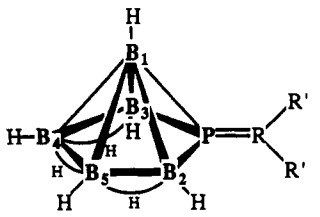

CLASS III

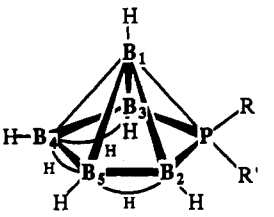

CLASS IV

43	R = C;	R' = H;	Charge = 0
44	R = C;	R' = CH_3;	Charge = 0
45	R = C;	R' = CH_3, CH_2F;	Charge = 0
46	R = C;	R' = CH_3, CH_2Cl;	Charge = 0
47	R = C;	R' = CH_2F, CH_2F;	Charge = 0
48	R = C;	R' = CH_2Cl, CH_2Cl;	Charge = 0
49	R = C;	R' = CH_2F, CHF_2;	Charge = 0
50	R = C;	R' = CH_2Cl, $CHCl_2$;	Charge = 0
51	R = C;	R' = CHF_2, CHF_2;	Charge = 0
52	R = C;	R' = $CHCl_2$, $CHCl_2$;	Charge = 0
53	R = C;	R' = CHF_2, CF_3;	Charge = 0
54	R = C;	R' = $CHCl_2$, CCl_3;	Charge = 0
55	R = C;	R' = CF_3;	Charge = 0
56	R = C;	R' = CCl_3;	Charge = 0
57	R = C;	R' = C_6H_5;	Charge = 0
58	R = C;	R' = $Si(CH_3)_3$;	Charge = 0
59	R = C;	R' = H; $Cr(CO)_3$	Charge = 0

60	R = H;	R' = H;	Charge = 0
61	R = CH_3;	R' = CH_3;	Charge = 0
62a	R = CH_3;	R' = CD_3;	Charge = 0
62b	R = CD_3;	R' = CH_3;	Charge = 0
63	R = CF_3;	R' = CF_3;	Charge = 0
64a	R = H;	R' = F;	Charge = 0
64b	R = F;	R' = H;	Charge = 0
65a	R = H;	R' = Cl;	Charge = 0
65b	R = Cl;	R' = H;	Charge = 0
66	R = F;	R' = F;	Charge = 0
67	R = Cl;	R' = Cl;	Charge = 0
68a	R = Cl;	R' = CH_3;	Charge = 0
68b	R = CH_3;	R' = Cl;	Charge = 0
69a	R = Cl;	R' = C_6H_5	Charge = 0
69b	R = C_6H_5;	R' = Cl	Charge = 0
70a	R = Cl;	R' = $C(H)(C_6H_5)_2$;	Charge = 0
70b	R = $C(H)(C_6H_5)_2$;	R' = Cl;	Charge = 0
71a	R = Cl;	R' = $C(H)(SiMe_3)_2$;	Charge = 0
71b	R = $C(H)(SiMe_3)_2$;	R' = Cl;	Charge = 0
72	R = nothing;	R' = $C(^tBu)(H)(OSiMe_3)$;	Charge = -1
73a	R = $SiMe_3$;	R' = $C(^tBu)(H)(OSiMe_3)$;	Charge = 0
73b	R = $C(^tBu)(H)(OSiMe_3)$;	R' = $SiMe_3$;	Charge = 0
74a	R = H;	R' = $C(^tBu)(H)(OSiMe_3)$;	Charge = 0
74b	R = $C(^tBu)(H)(OSiMe_3)$;	R' = H;	Charge = 0
75a	R = H;	R' = $C(^tBu)(H)(OSiMe_3)$;	Charge = -1
75b	R = $C(^tBu)(H)(OSiMe_3)$;	R' = H;	Charge = -1
76	R = H;	R' = H; $Cr(CO)_3$	Charge = 0

Planes: Plane 1 = B(2), B(3), B(4), B(5)
Plane 2 = B(2), P, B(3)
Plane 3 = P, R, R'
Plane 4 = B(1), B(2), B(3)

Scheme IV. Synthetic Relationships between Class II Bridged and Class III Inserted Small Phosphaborane Systems

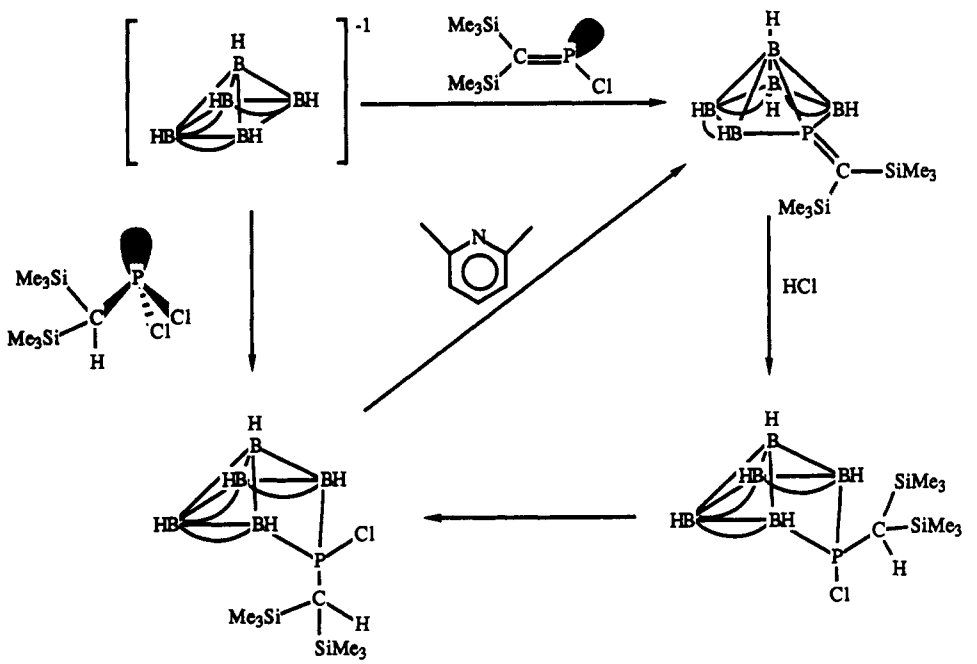

compound, [μ-((R)(Me_3SiO)C=P)B_5H_8] (where R = ^{t}Bu or adamantyl).[1] There are several reported members of the class II family.[1,44-47] In addition, we have demonstrated that it is possible to chemically convert a class II compound into a class I compound as shown in Scheme II. While their syntheses have been reported, very little is known about the structural, chemical, or electronic properties of either of these classes of compounds. Compounds belonging to classes III and IV are the related cage-inserted analogues of the class I and II compounds, inserted $B_5H_8P{=}CR_2$ (class III) and inserted $B_5H_8PR_2$ (class IV) compounds. The general structures of selected compounds belonging to classes III and IV are shown in Scheme III, and the data are reported in Tables II and III. The only known example of a class III compound has recently been reported by Gaines.[47] This species was prepared by either the dehydrohalogenation of the class I compound, μ-($(Me_3Si)_2HCP(Cl)$)B_5H_8, with base or the direct insertion of a chlorophosphaalkene into a pentaborane cage framework. The structure of this new species has been postulated as a cage-inserted compound on the basis of ^{11}B and ^{31}P NMR and mass spectroscopic data. The relationship and interconversion between class II and III systems is shown in Scheme IV. The final class of compounds, inserted $B_5H_8PCR_2$, represents a possible inserted phosphacarborane product from the reaction of phos-

Table II. Selected MNDO-Calculated Structural Data for Bridged and Inserted Phosphaborane Systems (Classes I–IV)

	bond distances, Å									bond angles, deg							planes,[a] deg		
class	B(1)–B(4,5)	B(1)–B(2,3)	B(2)–B(3)	B(2,3)–B(5,4)	B(4)–B(5)	B(2,3)–P	B(1)–P	P–R	P–R′	B(2)–B(1)–B(3)	B(2,3)–B(1)–B(5,4)	B(2,3)–P–R′	B(2,3)–B(5,4)–B(4,5)	B(1)–B(2,3)–P	B(2)–P–B(3)	R–P–R′	Pl(1)–Pl(2)	Pl(1)–Pl(3)	Pl(1)–Pl(4)
I (av)	1.812	1.661	2.564	1.936	1.781	1.922	2.483	1.589		100.7	67.7	204.8	101.7	87.4	83.4		129.2	89.6	56.1
9	1.813	1.656	2.516	1.955	1.777	1.916	2.534	1.569		98.9	68.4	202.5	100.9	89.5	82.1		125.5	91.0	55.1
10	1.812	1.653	2.504	1.955	1.782	1.916	2.527	1.589		98.5	69.0	198.5	100.6	89.9	81.7		125.4	89.9	54.5
11	1.813	1.656	2.525	1.948	1.777	1.920	2.518	1.588		99.3	68.1	203.0	101.1	89.3	82.2		126.1	89.5	55.0
13	1.841	1.660	2.549	1.935	1.773	1.924	2.502	1.585		100.3	67.6	204.5	101.6	88.3	83.1		128.0	89.5	56.0
15	1.814	1.663	2.575	1.924	1.772	1.925	2.480	1.583		101.5	67.0	206.2	102.1	87.1	83.9		129.6	89.8	57.2
17	1.814	1.666	2.603	1.910	1.772	1.926	2.455	1.584		102.7	66.4	208.2	102.6	85.8	85.0		131.5	91.0	57.8
19	1.814	1.668	2.630	1.899	1.775	1.931	2.430	1.590		104.0	66.0	209.5	103.0	84.6	85.8		133.1	91.0	58.3
21	1.806	1.670	2.648	1.891	1.776	1.935	2.412	1.593		104.9	65.6	211.1	103.3	83.7	86.4		134.0	91.0	58.5
II (av)	1.818	1.647	2.501	1.950	1.757	1.967	2.580	1.751	1.755	98.9	68.5	136.2	101.0	90.5	78.9	104.5	128.5	90.4	56.1
26	1.814	1.650	2.471	1.959	1.778	1.937	2.586	1.339	1.340	97.0	68.7	137.0	100.2	91.9	79.3	102.8	125.1	90.0	55.0
27	1.810	1.641	2.426	1.978	1.787	1.966	2.653	1.770	1.766	95.3	69.7	133.4	99.3	94.3	76.2	108.0	124.9	90.4	54.0
III (av)	1.738	1.868	3.040	1.775	1.676	1.972	2.024	1.594		107.3	58.8	186.6	112.0	63.6	99.4			90.2	63.7
43	1.702	1.904	3.110	1.792	1.640	2.003	2.018	1.575		109.6	59.3	191.2	114.2	62.2	101.9			89.5	62.6
44	1.703	1.902	3.104	1.789	1.640	2.002	2.021	1.599		109.4	59.2	191.1	114.2	62.3	101.7			90.9	63.0
IV (av)	1.703	1.860	3.042	1.779	1.662	2.036	2.097	1.760	1.771	109.7	59.6	123.1	112.8	64.6	95.7	104.2		90.4	62.4
60	1.694	1.893	3.108	1.793	1.645	2.033	2.052	1.340	1.344	110.4	59.7	118.0	114.1	62.9	99.7	105.5		90.4	61.8
61	1.689	1.883	3.101	1.792	1.647	2.064	2.090	1.776	1.782	110.9	59.9	117.5	113.9	63.8	97.4	107.2		91.5	62.0

[a] Plane 1 = B(2), B(3), B(4), B(5); plane 2 = B(2), P, B(3); plane 3 = P, R, R′; plane 4 = B(1), B(2), B(3). The angle reported between planes are indicated as

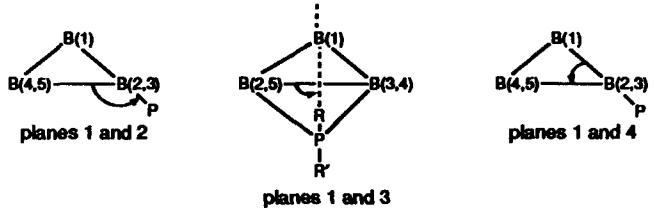

Table III. Selected MNDO-Calculated Electronic and Thermodynamic Data for Bridged and Inserted Phosphaborane Systems (Classes I–IV)

			charge distributions (e)												
											terminal H			bridging H	
class	ΔH_f, kJ mol^{-1}	IP, eV	B(1)	B(2)	B(3)	B(4)	B(5)	P	R	R′	$H_{B(2,3)}$	$H_{B(4,5)}$	$H_{B(1)}$	$H_{B(2-5)}$, $H_{B(3,4)}$	$H_{B(4,5)}$
I (av)	−215.55	10.11	−0.318	+0.182	+0.174	−0.044	−0.043	−0.063	−0.176		+0.006	+0.026	+0.055	−0.010	+0.070
9	109.80	9.94	−0.324	+0.211	+0.211	−0.053	−0.053	−0.253	+0.074		−0.009	+0.015	+0.045	−0.019	+0.065
10	30.94	9.77	−0.331	+0.217	+0.220	−0.056	−0.055	−0.242	−0.004		−0.012	+0.045	+0.045	−0.022	+0.064
11	−143.57	9.92	−0.321	+0.196	+0.202	−0.050	−0.050	−0.195	−0.065		−0.008	+0.018	+0.047	−0.017	+0.066
13	−318.23	10.12	−0.313	+0.194	+0.177	−0.043	−0.050	−0.137	−0.137		−0.003	+0.023	+0.052	−0.014	+0.068
15	−504.24	10.33	−0.306	+0.168	+0.177	−0.044	−0.043	−0.062	−0.201		+0.004	+0.028	+0.056	−0.011	+0.071
17	−689.65	10.38	−0.303	+0.130	+0.176	−0.045	−0.034	+0.034	−0.282		+0.013	+0.033	+0.060	−0.003	+0.073
19	−878.03	10.47	−0.304	+0.138	+0.150	−0.043	−0.034	+0.116	−0.331		+0.025	+0.036	+0.065	+0.003	+0.077
21	−1073.5	10.68	−0.303	+0.114	+0.155	−0.045	−0.024	+0.154	−0.354		+0.031	+0.040	+0.071	+0.007	+0.081
II (av)	−291.22	9.61	−0.337	+0.185	+0.166	−0.063	−0.060	−0.107	+0.050	+0.029	−0.001	+0.015	+0.046	−0.021	+0.068
26	58.04	10.46	−0.333	+0.209	+0.207	−0.056	−0.057	−0.199	+0.092	+0.059	−0.007	+0.018	+0.045	−0.026	+0.063
27	−93.58	10.36	−0.348	+0.235	+0.235	−0.061	−0.061	−0.320	+0.010	+0.082	−0.011	+0.014	+0.045	−0.030	+0.063
III (av)	−125.81	9.78	+0.040	−0.114	−0.122	−0.040	−0.042	+0.011	−0.163	+0.327	+0.036	+0.036	+0.004	+0.025	+0.054
43	177.78	9.85	+0.138	−0.135	−0.145	−0.073	−0.078	−0.206	+0.135	+0.060	−0.024	−0.024	+0.138	+0.010	+0.056
44	101.16	9.59	+0.140	−0.155	−0.140	−0.081	−0.074	−0.194	+0.056	+0.022	+0.022	+0.022	+0.140	+0.010	+0.056
IV (av)	−197.85	9.37	+0.053	−0.131	−0.118	−0.077	−0.092	−0.039	+0.112	+0.035	+0.027	+0.027	+0.053	+0.010	+0.045
60	121.20	10.34	+0.140	−0.151	−0.151	−0.082	−0.082	−0.150	+0.121	+0.117	−0.012	−0.012	+0.140	+0.071	+0.074
61	−23.05	10.13	+0.133	−0.144	−0.144	−0.081	−0.080	−0.230	+0.114	+0.117	+0.027	+0.027	+0.133	−0.005	+0.041

Scheme V. Inserted Phosphacarborane Systems

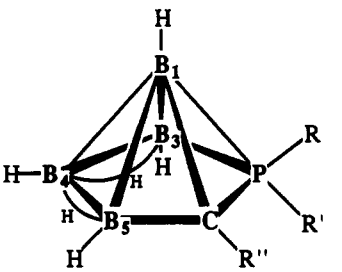

CLASS V

77	R =	nothing;	R′ =	nothing;	R″ =	H;	Charge =	0
78	R =	nothing;	R′ =	nothing;	R″ =	CH_3;	Charge =	0
79	R =	nothing;	R′ =	nothing;	R″ =	(CH_2CH_3);	Charge =	0
80	R =	nothing;	R′ =	nothing;	R″ =	$C(CH_3)_3$;	Charge =	0
81	R =	nothing;	R′ =	nothing;	R″ =	CF_3;	Charge =	0
82	R =	H;	R′ =	H;	R″ =	H;	Charge =	0
83	R =	CH_3;	R′ =	CH_3;	R″ =	CH_3;	Charge =	0
84	R =	(CH_2CH_3);	R′ =	(CH_2CH_3);	R″ =	(CH_2CH_3);	Charge =	0
85	R =	$C(CH_3)_3$;	R′ =	$C(CH_3)_3$;	R″ =	$C(CH_3)_3$;	Charge =	0
86	R =	CF_3;	R′ =	CF_3;	R″ =	CF_3;	Charge =	0
87	R =	nothing;	R′ =	nothing;	R″ =	H;	Charge =	-1
88	R =	nothing;	R′ =	nothing;	R″ =	CH_3;	Charge =	-1
89	R =	nothing;	R′ =	nothing;	R″ =	(CH_2CH_3);	Charge =	-1
90	R =	nothing;	R′ =	nothing;	R″ =	$C(CH_3)_3$;	Charge =	-1
91	R =	nothing;	R′ =	nothing;	R″ =	CF_3;	Charge =	-1

phaalkynes with pentaborane(9).[4] These systems are shown in Scheme V. Complete data for this final class of phosphaboranes (and for all classes of compounds) are available as supplemental material.

For all 91 compounds calculated, the geometry-optimized systems corresponded well with the proposed structures of analogous reported compounds (on the basis of spectroscopic analyses).[1,44-47] All bond lengths and angles were also found to be within the normal range for those reported in crystallographically determined borane, carborane, and large phosphaborane systems.

Class I and II Systems. The general minimum energy structures for class I compounds are based on a modified pentaborane(9) framework in which one bridging hydrogen atom has been subrogated by a phosphino group. In the calculations, the phosphorus atom was initially input in the basal plane containing boron atoms B(2–5). The phosphine groups were displaced by the calculation from this coplanar configuration to underneath the open nido face of the cage, forming a dihedral angle of between 46.0 and 56.1° (Table II). The exopolyhedral R′–R–R′ plane is approximately coparallel with the B(2)–P–B(3) plane, as anticipated on the basis of the required orbital stereochemistry of the P=C interaction. The projection of the apical boron atom on the basal plane is significantly displaced from the centroid of the four boron atom basal plane toward the phosphorus atom. This can be seen from the variation in the bond distances between the apical boron and the basal boron atoms B(4,5) (1.81 Å) and the apical to basal boron atoms B(2,3) (1.66 Å). In addition, the B(2)–B(3) bond distances are significantly longer in class I compounds (2.43–2.63 Å) than for pentaborane(9) (1.86 Å calculated, 1.70 Å experimental).[50] This is consistent with the proposed B–P–B interaction as consisting

(50) (a) Dulmage, W. J.; Lipscomb, W. N. *J. Am. Chem. Soc.* **1951**, *73*, 3539. (b) Dulmage, W. J.; Lipscomb, W. N. *Acta. Crystallogr.* **1952**, *5*, 260. (c) Hedberg, K.; Jones, M. E.; Schomaker, V. *J. Am. Chem. Soc.* **1951**, *73*, 3538. (d) Hedberg, K.; Jones, M. E.; Schomaker, V. *Proc. Natl. Acad. Sci.* **1952**, *38*, 679. (e) Hrostowski, H. J.; Myers, R. J.; Pimentel, G. C. *J. Chem. Phys.* **1952**, *20*, 518.

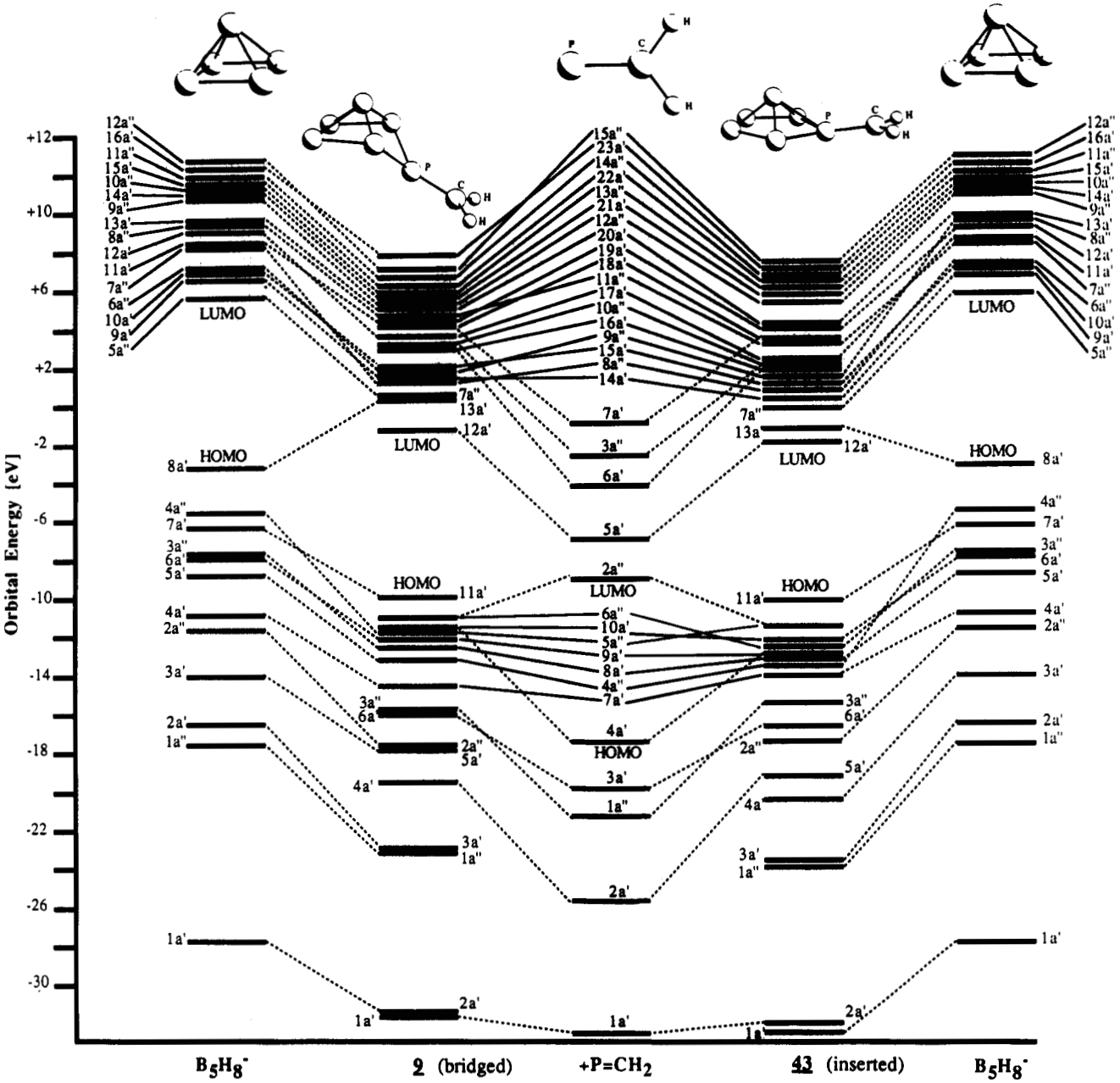

Figure 2. Molecular orbital correlation diagram for bridged (9) and inserted (43) $B_5H_8P{=}CH_2$ systems.

of two 2-center-2-electron bonds for bridged phosphapentaborane systems rather than consisting of a single 3-center-2-electron bonding scheme.[1,44-47] The structure is formally derived from a 2-electron reduction of a *nido*-pentaborane structure by the 3-electron-donating phosphino unit to produce an *arachno*-pentaborane structure that is directly analogous to *arachno*-B_5H_{11}.

The orbital energies for the prototypic class I compound, bridging $B_5H_8P{=}CH_2$, are shown in the molecular orbital correlation diagram in Figure 2. Group orbital connectivities between the orbitals of **9** and those from the $B_5H_8^-$ and $P{=}CH_2^+$ fragments were assigned on the basis of the LCAO orbital contributions, orbital population analysis, and orbital symmetry (the noncrossing rule was observed except where significant orbital mixing occurs in adjacent intermediate orbitals). The cage framework has overall C_s symmetry, and as such, the molecular orbitals for **9** are either symmetric (a′) or antisymmetric (a″) with respect to the mirror plane. The molecule has 17 filled and 21 virtual orbitals of which 11 are primarily intracage interactions, 2 are PCH_2 interactions, and 4 are primarily cage-phosphorus fragment interactions. The five highest occupied and two lowest unoccupied orbitals are shown in Figure 3. The HOMO, orbital 11a′, and orbital 10a′ are both P–C bonding orbitals but are also phosphorus–apical boron antibonding and bonding orbitals, respectively. The major atomic contributions to the HOMO orbital are the B(1) p_y (20.8%), the phosphorus p_x (19.3%), and the carbon p_x (19.3%) orbitals. Orbitals 5a″ and 6a″ are predominantly cage-phosphorus fragment bonding orbitals with large contributions from the phosphorus p_z orbital. The two lowest energy virtual orbitals, 12a′ and 13a′, are primarily phosphorus–carbon antibonding in nature.

The relationship between bridging and inserted structures for small phosphaborane compounds is of particular interest for both theoretical and experimental considerations. An indepth understanding of the relationships between bridged and inserted phosphaborane structures first requires a detailed knowledge of the electronic structures of these systems. The variation in the orbital energies as a function of the bridging dihedral angle is shown in Figure

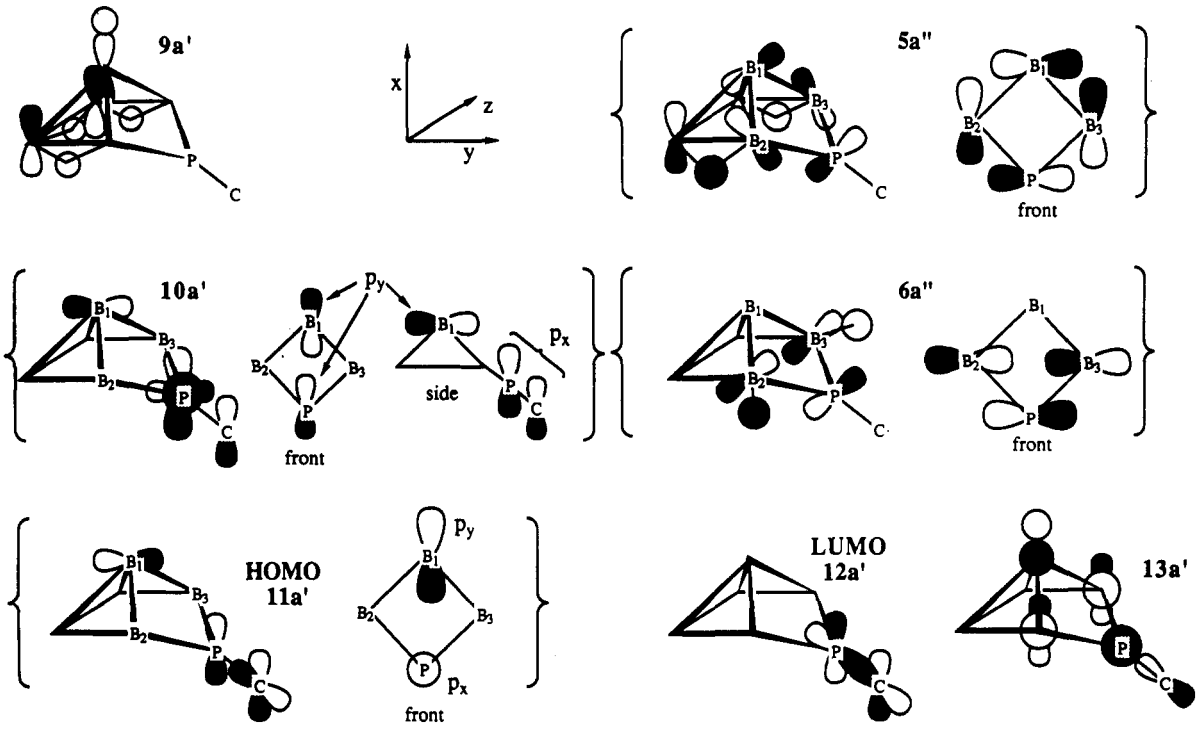

Figure 3. Selected molecular orbitals for class I compounds (bridged $B_5H_8P{=}CR_2$).

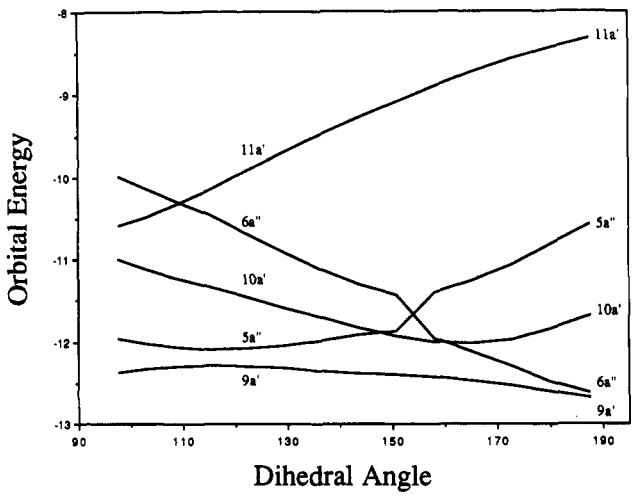

Figure 4. Molecular orbital energy dependence (eV) on the dihedral angle (deg) for class I compounds (bridged $B_5H_8P{=}CR_2$).

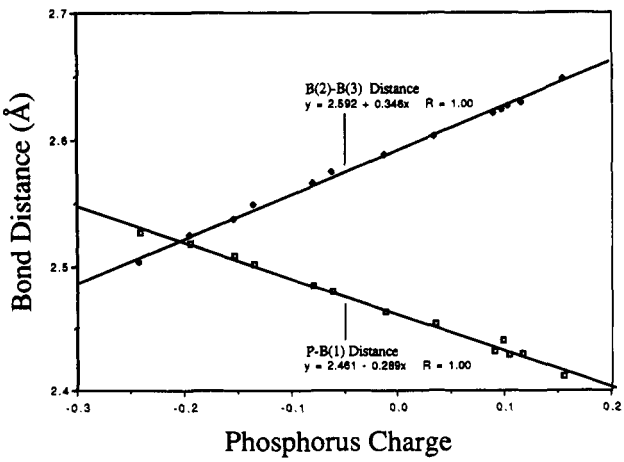

Figure 5. Dependence of P–B(1) and B(2)–B(3) bond distances (Å) on the charge at phosphorus (e) for class I compounds (bridged $B_5H_8P{=}CR_2$).

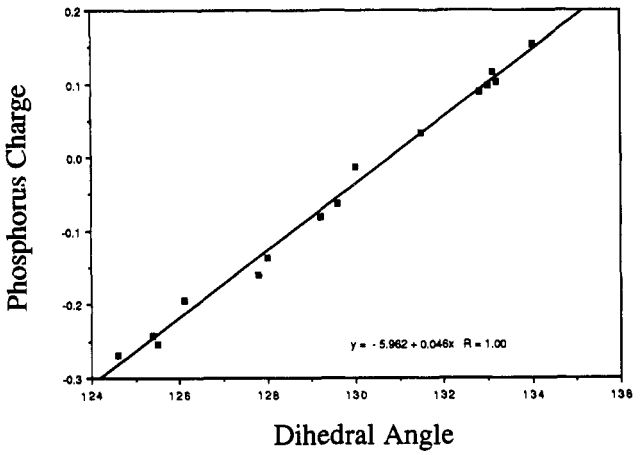

Figure 6. Dependence of the [B(2–4) basal plane]–[B(2)–P–B(3) plane] dihedral angle (deg) on the calculated charge on phosphorus (e) for class I compounds.

4. As the structure changes from a bridging case toward the inserted geometry, the HOMO shifts to significantly higher energy. This increase in energy is due primarily to the increased antibonding interaction between the phosphorus p_x orbital and the apical boron p_y orbital. The next lowest energy orbital, 6a″, moves to lower energy due to a large increase in the bonding overlap integral between the phosphorus p_z and the two bridged basal boron p_z orbitals. The 10a′ orbital moves to slightly lower energy upon an increase in the dihedral angle because of a more favorable overlap between the phosphorus p_z and the apical boron p_y orbital. The 5a″ orbital shifts to higher energy upon increasing the dihedral angle because of a decrease in the bonding overlap between the phosphorus p_z orbital and the two basal boron cage bonding orbitals. Simultaneously, an increase in the phosphorus–apical boron antibonding interaction occurs. These two contributions result in the MO shifting to higher energy.

An interesting linear relationship was observed between the calculated charge on phosphorus and the P–B(1) and

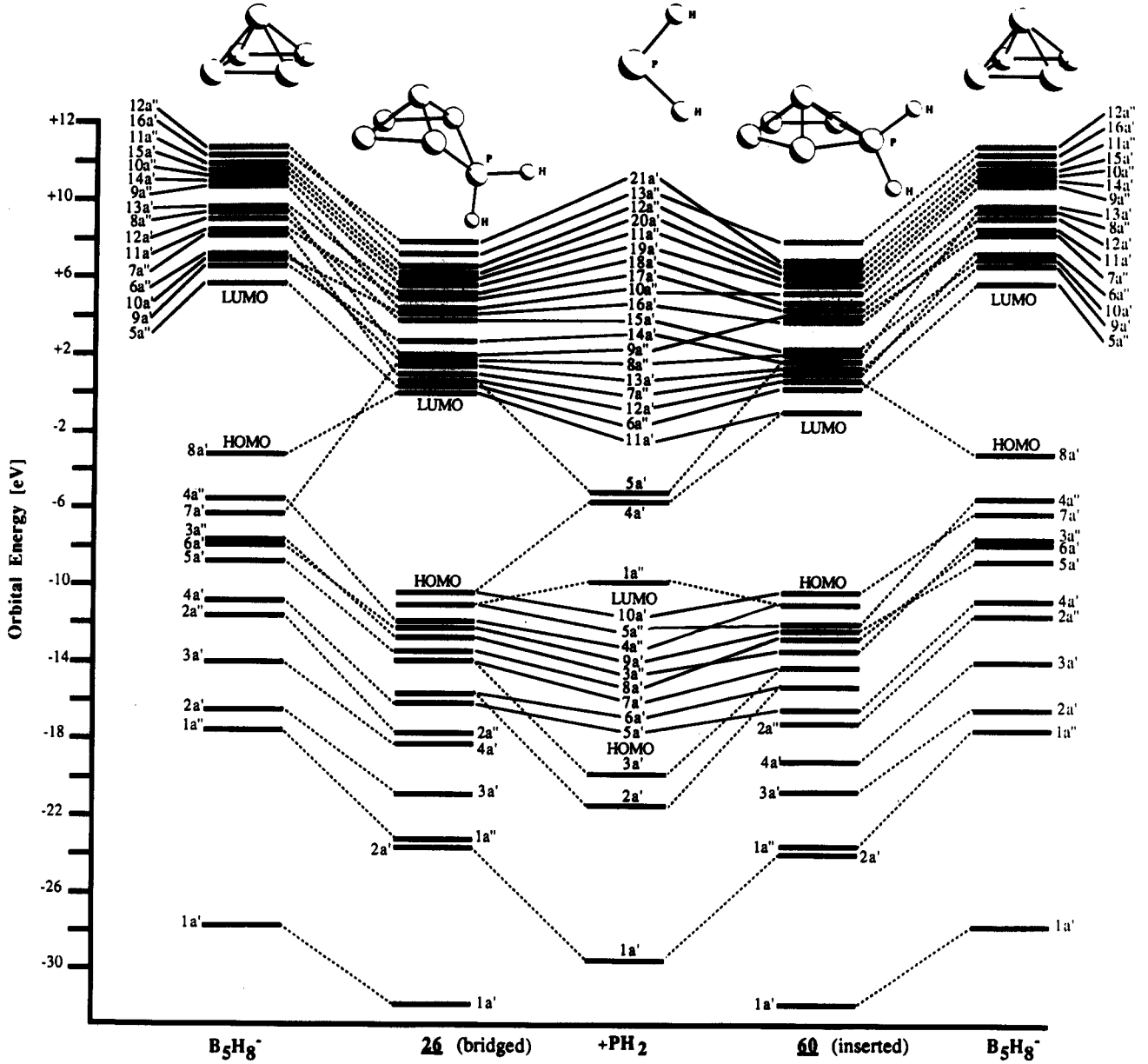

Figure 7. Molecular orbital correlation diagram for bridged (**26**) and inserted (**60**) $B_5H_8PH_2$ systems.

the B(2)–B(3) bond distances. The charge on the phosphorus atom was systematically varied by halogen substitution on peripheral methyl groups $B_5H_8P{=}C(CH_{3-n}X_n)_2$ (where X = F or Cl and n = 0–3). As the phosphorus charge increases, the optimized minimum energy structure shifts toward the inserted case, as shown in Figure 5. As a result, the phosphorus–apical boron bond distance decreases. The bond distance between the two bridged basal boron atoms increases primarily due to an expansion of the basal ring from four to five vertices. This structural trend toward an inserted cage upon increasing the phosphorus charge can also be seen clearly from the plot of the calculated charge on phosphorus versus the [B(2–4) basal plane]–[B(2)–P–B(3) plane] dihedral angle. This relationship is shown in Figure 6. This result is primarily due to a significant stabilization of the 6a″ orbital and a destabilization of the 11a′ orbital. The sum of the energies of the other occupied MOs in the inserted structure also shift slightly to overall lower energy as the phosphorus charge increases.

The calculated structures of class II compounds are similar to those of class I except that the $P{=}CR_2$ group has been replaced with a PRR′ group. The PRR′ plane is approximately perpendicular to the basal B(2–5) plane with one R group directed below the nido face of the cage and the other directed above and away from the open face. As a result, compounds belonging to class II (and also class IV) can exhibit exo–endo isomerization, depending on the barrier to B–P–B rotation.[51] It has been experimentally observed that the barriers to rotation separating the two isomers are sufficiently small in several systems such that room-temperature interconversion of the two isomers has been observed.[44-46] In the majority of cases in which endo–exo isomerization is possible, the most stable isomer was found by MNDO calculations to be the one in which the most electronegative group was directed under the open face of the cage in the endo position (R′ of Scheme I).

The MO group correlation diagram for the prototype compound for class II, bridging $B_5H_8PH_2$ (**26**), is shown in Figure 7. The individual LCAO orbitals for this system

(51) The endo isomer is defined as that isomer having the sterically most demanding group directed under the open face of the cage, which is the a isomer. The exo isomer, with the larger group directed above the cage, is listed as the b isomer.

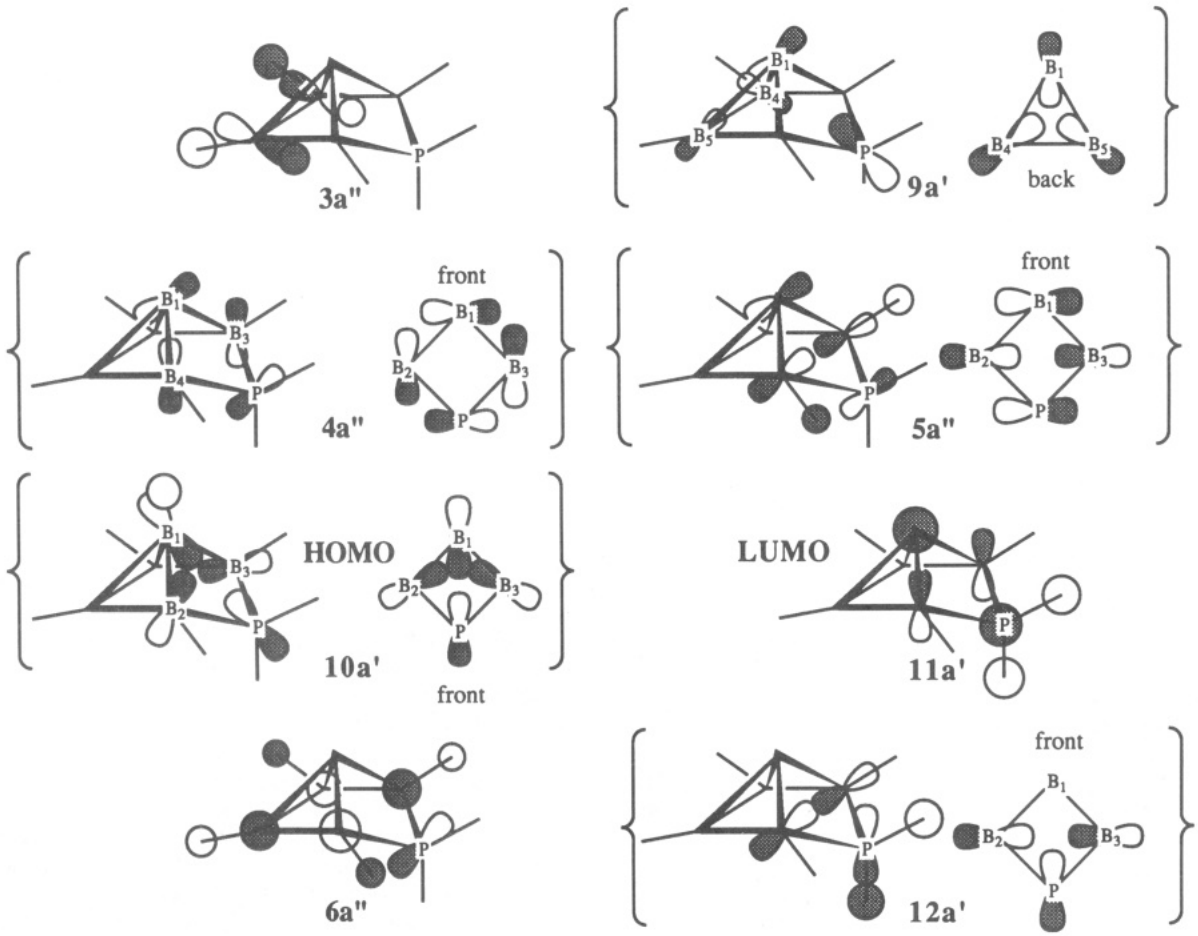

Figure 8. Selected molecular orbitals for class II compounds (bridged $B_5H_8PR_2$).

are shown in Figure 8. The molecule has 15 filled and 19 virtual orbitals. The HOMO in this system, orbital 10a′, is apical boron-bridged basal boron bonding and phosphorus-cage antibonding in character. The major contributions to this orbital are a bonding set from B(1–3) (52.4%) and a phosphorus p_y relative antibonding orbital (16.9%). Orbitals 4a″ and 5a″ are the in-plane and out-of-plane B(1–3)–phosphorus bonding orbital set, which contain significant phosphorus p_z contributions (32.5 and 24.9%, respectively). These orbitals are qualitatively similar to orbitals 5a″ and 6a″ in compound **9**, respectively.

As was observed for class I compounds, there is a strong orbital energy dependence on the bridging dihedral angle in class II systems as shown in Figure 9. There is also a qualitative similarity in the angular dependence of the orbital energies for class I and II compounds. Orbital 10a′ increases in energy and orbital 5a″ decreases in energy as the structure moves toward the inserted structure. Other orbitals for compound **26** show a relationship similar to those of class I.

The sums of the orbital energies for the lowest 12 occupied MOs for compound **26** are −221.62 eV for a 95° dihedral angle and −221.44 eV for 180° ($\Delta = |\sum_{95°}$ orbital energy $- \sum_{180°}$ orbital energy$| = 0.18$ eV). These values represent the largest variation across the range of angles, with intermediate values showing less angular dependence on the dihedral angle. This compares with the variation in the sums of the highest three occupied MOs, which are −33.53 for 95° and −32.36 for 180° ($\Delta = 1.17$ eV). The relatively small variation in the sum of the first 12 orbital energies and the relatively large variation in the sum of the three highest energy orbitals as a function of dihedral angle clearly indicate that the relationship between the

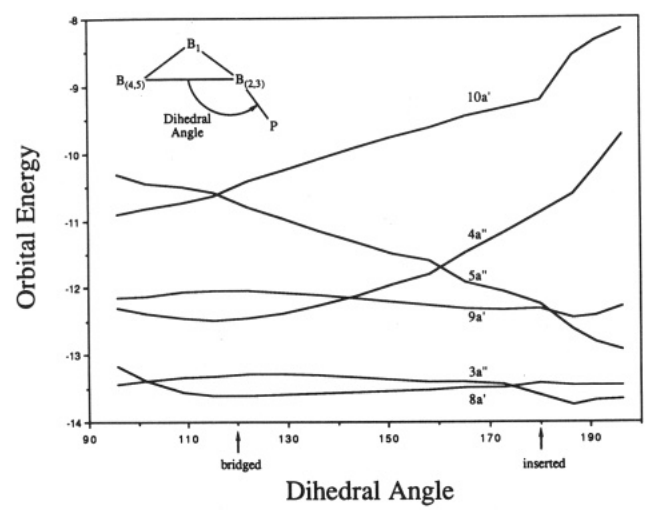

Figure 9. Molecular orbital energy dependence (eV) on the dihedral angle (deg) for class II compounds (bridged $B_5H_8PR_2$).

highest three orbitals accurately reflects the total energy variation for the molecule as a function of the bridging dihedral angle. This relationship can thus be used to gain a clearer understanding of the orbital factors leading to the stabilization or destabilization of a particular geometry. Among the three highest MOs, the 4a″ orbital appears to be the most sensitive probe of the relative overall orbital energy as a function of the dihedral angle, since the energy contributions from the 10a′ and 5a″ orbitals approximately cancel each other ($\sum$ orbital energies for the lowest 12 and the 5a″ and 10a′ orbitals = −242.84 eV for 95° and −242.92 eV for 180° ($\Delta = -0.08$ eV); 4a″ orbital energy = −12.31

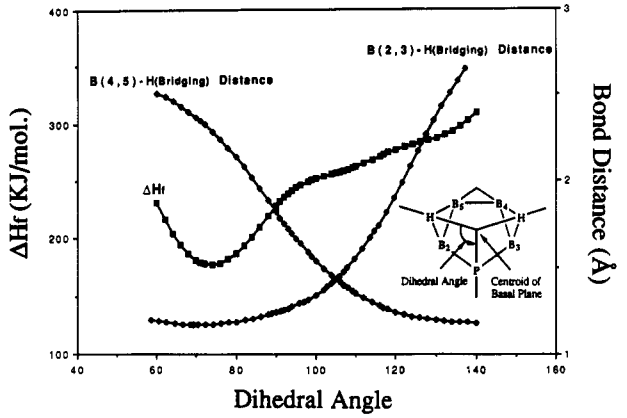

Figure 10. Bridging proton–basal cage boron distance and heat of formation dependence on dihedral angle (deg) for class III compounds ($B_5H_8P{=}CH_2$ inserted systems).

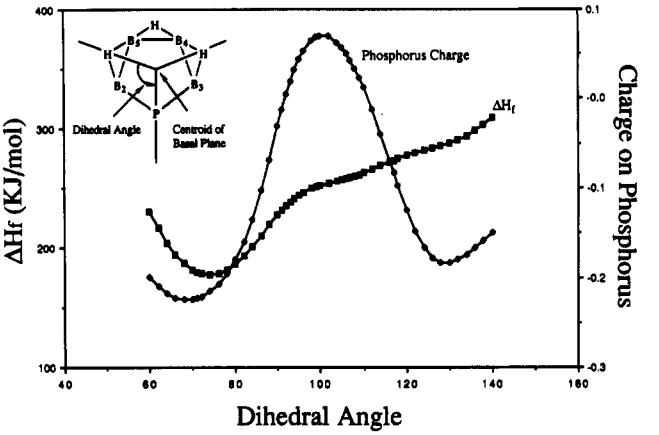

Figure 11. Phosphorus charge (e) and heat of formation dependence on dihedral angle (deg) for class III compounds ($B_5H_8P{=}CH_2$ inserted systems).

eV for 95° and −10.89 eV for 180° (Δ = 1.42 eV). As the structure is changed from a bridged to an inserted system, the 4a″ orbital is strongly destabilized due to an attenuation of the P–B(2,3) bonding interaction to an essentially nonbonding situation and to an increase in the P–B(1) antibonding interaction.

Classes III and IV. The structures of class III and class IV compounds are based on a pentagonal-pyramidal system. The relationship between the orbitals for class III compounds and those of class I is shown in Figure 2, as previously discussed.

An interesting relationship was observed for the calculated positions of the bridging hydrogen atoms in class III compounds. In the freely varied structure, the hydrogens bridging the basal boron atoms B(2,3) and the back-basal boron atoms B(4,5) are shifted away from the symmetrically bridged situation toward a terminal position on the B(2,3) boron atoms. The variations in the calculated heat of formation and in the basal boron-bridging hydrogen-bond distances with the dihedral-bridging hydrogen angle are shown in Figure 10 (the dihedral bridging hydrogen angle is defined here as the angle formed between the bridging hydrogen atom, the centroid of the basal five-membered plane, and the phosphorus atom, as shown in the figure). The symmetrically bridged case, the point of intersection between the B(4,5)-bridging hydrogen distance and the B(2,3)-bridging hydrogen distances curves, occurs at approximately 108°. While there is a small inflection in the ΔH_f curve at approximately that point, the overall minimum energy structure occurs at a dihedral angle of approximately 73°. Two small inflections at significnatly higher energies were observed in the ΔH_f versus dihedral angle curves corresponding to the symmetrically bridged case and to the structure in which the hydrogen atoms have shifted to the nonphosphorus-bridged basal boron atoms. The calculated charge on the phosphorus atom and the B(4,5) basal boron atoms remains essentially constant from the bridged to the inserted structure. In addition, the apical boron atom becomes much more positive and the B(2,3) boron atoms more negative with this structural change. The shift of the hydrogen from a bridging position to a B(2,3) terminal position results in the shift of a significant amount of the calculated electron density from the apical boron (calculated charge on B(1) in the symmetrically bridged structure = −0.244 e and the charge in the terminal hydrogen structure = +0.138 e) to the phosphorus atom (symmetrically bridged charge = +0.034 e, terminal charge = −0.206 e) and the basal boron atoms it bridges (average symmetrically bridged charge = +0.035 e, average terminal charge = −0.140 e). This relationship between dihedral angle and calculated charge at phosphorus is shown in Figure 11.

The shift of bridging hydrogen atoms along an open nido face of a phosphaborane system, as described above for Class III compounds, from the symmetrically bridged situation to an asymmetrically bridged case has been observed experimentally. In the X-ray structure for $B_{10}H_{10}PCH_3$ (6) the protons bridging the nido face of the cage are shifted away from the phosphorus atom and toward the non-phosphorus-bonded boron atoms.[10] These asymmetric bridges have short bond lengths of 1.14 Å and long bond lengths of 1.33 Å. This same asymmetric shift was found in the calculated structure for 6, in which the calculated minimum energy structure shifted the bridging hydrogen atoms away from the phosphorus atom by approximately 0.10 Å. The ability of the MNDO calculational method to accurately reflect these subtle structural variations further supports the utility of this method in providing valuable information in these heteroborane cluster systems.

Class V. The final class of small phosphaborane systems studied were the side-inserted $R'_2PCRB_4H_6$ systems. Compounds of this type are a possible product from the reaction of low-valent phosphorus compounds with borane cluster compounds.[4] Specific questions of practical interest in these systems are how the lone pair of electrons on the phosphorus atom (where R′ = nothing; 77) will behave and whether or not they will be available for exopolyhedral organometallic complex formation. The lone pair of electrons was found to be significantly mixed with cage bonding orbitals in the third highest MO (38.3% phosphorus character). The calculated charge on the phosphorus was +0.358 e. Formation of the anion of 77, complex 87, shifts the lone pair to the second highest MO with significantly less cage orbital mixing. The calculated charge density on the phosphorus was found to be −0.067 e for 87. These data support the conclusion that the lone pair of electrons on the phosphorus is significantly involved in cage bonding in the neutral system and is not readily available for exopolyhedral coordination, but that these electrons should be accessible in the deprotonated anionic system.

Acknowledgment. We wish to thank the National Science Foundation (Grant No. MSS-89-09793), the donors of the Petroleum Research Fund, administered by the American Chemical Society, the General Electric Co., the Rome Air Development Center (Award No. F30602-89-C-0113), IBM, and the Industrial Affiliates Program of the

Center for Molecular Electronics for support of this work. We also wish to thank Prof. Robert R. Birge and Prof. Teresa B. Freedman for their assistance with this work.

Supplementary Material Available: Tables of complete MNDO-calculated bond lengths, bond angles, interplane dihedral angles, energy terms (electronic and thermodynamic data), and internal charge distribution data for compounds belonging to classes I–V (17 pages). Ordering information is given on any current masthead page.

Small Heteroborane Cluster Systems. 2.[1] Preparation of Phosphaborane Systems from the Reaction of Small Borane Cages with Low-Coordinate Phosphorus Compounds: Reaction Chemistry of Phosphaalkenes with Pentaborane(9)

Robert W. Miller, Kelley J. Donaghy, and James T. Spencer*

Department of Chemistry and Center for Molecular Electronics, Center for Science and Technology, Syracuse University, Syracuse, New York 13244-4100

Received August 29, 1990

The reaction of $(Me_3Si)P{=}C(R)(OSiMe_3)$ (where R = *tert*-butyl (**1a**) or adamantyl (**1b**)) with 1 equiv of neutral pentaborane(9), B_5H_9, under mild conditions produces the synthetically versatile, small bridging phosphaboranes $[\mu\text{-}((R)(Me_3SiO)HCP(SiMe_3))B_5H_8]$ (**2a,b**) in excellent yields. Two possible mechanisms for the formation of **2a** and **2b** by this reaction are supported by both experimental and MNDO semiempirical theoretical data. These relatively thermal and air-stable compounds are also stable with respect to the elimination of $Me_3SiOSiMe_3$. They are quantitatively converted, however, to $[\mu\text{-}((R)(Me_3SiO)CHP(X))B_5H_8]$ (where X = H (**3a,b**) and X = D (**4a,b**)) by electrophilic substitution reactions with water, D_2O, or alcohol. Compound **2a** is readily bridge-deprotonated by the action of NaH to produce the corresponding anion, $[\mu\text{-}((tert\text{-butyl})(Me_3SiO)CHP(SiMe_3))B_5H_7]^-$ (**5a**), while **2b** is unreactive under similar conditions. Compound **5a** was found to be unreactive toward metal cations in complex formation. Compound **3a** slowly loses H_2 on standing at room temperature to form the bridged P=C system, $[\mu\text{-}((tert\text{-butyl})(Me_3SiO)C{=}P)B_5H_8]$ (**6a**). Compound **3a** is readily cage-deprotonated to form the corresponding anion, $[\mu\text{-}((tert\text{-butyl})(Me_3SiO)CHP(H))B_5H_7]^-$ (**7a**), which, when reacted with metal halides, forms metallaphosphaborane complexes. Data from MNDO calculations for compounds **2a**, **3a**, **5a**, and **6a** show linear relationships between the calculated charge on the bridgehead boron atoms and both the phosphorus–apical boron bond distance and the bridgehead basal boron bond centroid–phosphorus–carbon bond angle. These trends have been rationalized by using semiempirical molecular orbital considerations. Characterization of the new compounds was by ^1H, ^{11}B, ^{13}C, and ^{31}P NMR, infrared, mass spectral, and elemental analyses.

Introduction

An understanding of the important chemical relationships between bridged and inserted structures in substituted molecular clusters requires a detailed knowledge of the electronic structures and chemical features affecting these types of clusters. One class of polyhedral compounds in which these contributing factors can be carefully examined are the small heteroborane systems (with fewer than nine vertex atoms), specifically the phosphaboranes, since both theoretical and synthetic tools are either available or can be developed for their study. While several large phosphaborane systems have been previously reported, relatively little work has been done with systems with fewer than nine vertex boron atoms. It has been clearly demonstrated that the chemistry of large borane systems is significantly different from that of the smaller cages. The only small phosphaborane systems that have thus far been reported are several μ-phosphinopentaboranes by Burg,[2,3a,4] Gaines,[5] and Spencer,[3b] the *closo*-$P_2B_4Cl_4$ system,[6a] a P_2B_3 cage,[6b] two $C_{2n}B_4P_4$ (where n = 1 or 2) cages,[6c] and an inserted phosphahexaborane structure reported by Gaines.[5] Several terminally substituted phosphine–pentaborane species have also been reported.[6d] In addition, little is known about the reaction chemistry of these heteroborane systems.

The application of compounds containing both group III and V elements within a single species to the formation of thin-film materials by chemical vapor deposition (CVD) is an area of intense current interest.[7] Boron phosphide is particularly important as a III–V semiconductor in thermoelectric devices due to its wide band gap, high thermal conductivity, and high chemical stability.[8] The new compounds reported in this paper are potentially useful as CVD source materials for the formation of boron phosphide thin films.

In this paper, we report the rational high-yield synthesis and reaction chemistry of a family of synthetically versatile small phosphaboranes from the reaction of low-valent phosphorus compounds with pentaborane(9). These systems exhibit a wide diversity of substitution and elimi-

(1) Part 1: Glass, J. A., Jr.; Whelan, T. A.; Spencer, J. T. *Organometallics*, preceding paper in this issue.
(2) Burg, A. B. *Inorg. Chem.* **1973**, *12*, 3017.
(3) (a) Burg, A. B.; Heinen, H. *Inorg. Chem.* **1968**, *7*, 1021. (b) Miller, R. W.; Donaghy, K. J.; Spencer, J. T. *Phosphorus, Sulfur Silicon Relat. Elem.* **1991**, *57*, 287.
(4) Mishra, I. B.; Burg, A. B. *Inorg. Chem.* **1972**, *11*, 664.
(5) Coons, D. E.; Gaines, D. F. *Inorg. Chem.* **1987**, *26*, 1985.
(6) (a) Haubold, W.; Keller, W.; Sawitzki, G. *Angew. Chem., Int. Ed. Engl.* **1988**, *27*, 925. (b) Wood, G. L.; Duesler, E. N.; Narula, C. K.; Paine, R. T.; Noth, H. *J. Chem. Soc., Chem. Commun.* **1987**, *496*. (c) Driess, M.; Pritzkow, H.; Siebert, W. *Angew. Chem., Int. Ed. Engl.* **1988**, *27*, 399. (d) Kameda, M.; Kodama, G. *Inorg. Chem.* **1987**, *26*, 2011.
(7) Dowben, P. A.; Spencer J. T.; Stauf, G. T. *Mater. Sci. Eng. B* **1989**, *B2*, 297.
(8) Kumashiro, Y. *Rigaku J.* **1990**, *7*, 21.

0276-7333/91/2310-1161$02.50/0